

Dynamic regimes in YBCO in applied magnetic field probed by swept frequency microwave measurements

This article has been downloaded from IOPscience. Please scroll down to see the full text article.

2004 J. Phys.: Condens. Matter 16 6969

(<http://iopscience.iop.org/0953-8984/16/39/029>)

View [the table of contents for this issue](#), or go to the [journal homepage](#) for more

Download details:

IP Address: 129.252.86.83

The article was downloaded on 27/05/2010 at 17:59

Please note that [terms and conditions apply](#).

Dynamic regimes in YBCO in applied magnetic field probed by swept frequency microwave measurements

S Sarti¹, E Silva², M Giura¹, R Fastampa¹, M Boffa³ and A M Cucolo³

¹ Dipartimento di Fisica and INFM, Università 'La Sapienza', Piazzale Aldo Moro 2, 00185 Roma, Italy

² Dipartimento di Fisica 'E. Amaldi' and INFM, Università 'Roma Tre', Via della Vasca Navale 84, 00146 Roma, Italy

³ Dipartimento di Fisica and INFM, Università di Salerno, Via S Allende-I, 84081 Baronissi, Salerno, Italy

Received 28 April 2004

Published 17 September 2004

Online at stacks.iop.org/JPhysCM/16/6969

doi:10.1088/0953-8984/16/39/029

Abstract

We report measurements of the microwave resistivity in $\text{YBa}_2\text{Cu}_3\text{O}_{7-\delta}$ (YBCO), in the presence of an applied magnetic field. Measurements are performed as a function of frequency, over a continuum spectrum between 6 and 20 GHz, by means of a Corbino disc geometry. These data allow for a direct identification of different dynamical regimes in the dissipation of YBCO in the presence of an applied magnetic field. While at high temperatures a frequency independent resistivity is observed, at lower temperatures we find a marked frequency dependence. The line in the (H, T) plane at which this change in the dynamical regime is observed is clearly identified and discussed in terms of vortex motion and fluctuational resistivity.

1. Introduction

Several dissipative mechanisms are known to participate to the overall resistivity of high T_c superconductors (HTSs) in an external magnetic field. Among them, the two major classes of phenomena are related to flux motion and thermal fluctuations. While a large number of papers have been published in the past regarding each of the two mechanisms [1], very few reports have dealt with the interplay of these two mechanisms and with the precise determination of the respective temperature and magnetic field applicability ranges [2]. Some indications from this point of view have been obtained from the analysis of dc resistivity data in presence of an applied magnetic field. In those cases, the above mentioned temperature and field ranges were typically identified by fitting the data with some model and looking for the ranges of validity of the model themselves. A more direct and natural experimental approach to this problem is to measure the resistive dissipation as a function of frequency. In this way, the different

dynamics of the two mechanisms can be experimentally tested, giving direct evidence for the dominating process.

Measurements as a function of frequency have been performed in the past either through multifrequency resonating structures (MFRs) [3], or through non-resonant techniques [4]. The advantage of the former is the high sensitivity that can be reached through this kind of set-up (typically down to $10^{-4}\rho_n$), compared to the relatively low sensitivity ($\simeq 10^{-2}\rho_n$) of the latter. On the other hand, MFRs allow for just a few fixed frequency measurements, while non-resonating techniques allow for measurements over a continuous frequency spectrum. Moreover, MFRs are practically realized through the patterning of the measured film to obtain appropriate stripline geometries, in which the microwave currents flow mainly near the border of the sample. As a result, the measurement is extremely sensitive to the response of the sample near the film border. This response can be rather different from the response of the interior, due both to possible damage of the film near the edge and to geometrical barriers that can affect vortex mobility.

In this paper, we present measurements performed through a Corbino disc geometry. Besides the possibility of a measurement over a continuous frequency spectrum, this geometry has the advantage of having current configurations that exclude spurious effects due to the sample edges: unlike other measuring geometries, currents are confined well inside the sample, and vortices, if present, move on circular orbits, never crossing the border of the sample. Due to the extreme difficulties that have to be faced in performing these experiments, we will present the experimental procedure in some detail, in order to clarify the hypothesis on which the measurement is based and the limit of validity of the experimental results. Next, we will show to what extent the microwave measurements can identify the two main dissipative mechanisms (vortex motion and fluctuations), through the different associated dynamics. We will show that two markedly different dynamical regimes can be directly identified through the data. While the low temperature regime can be interpreted in terms of constrained vortex motion, the high temperature regime is compatible with both vortex free flow and fluctuations.

2. Experimental set-up and samples

In the Corbino disc geometry the sample shortcircuits a coaxial cable. The measured quantity is the reflection coefficient of the microwave line, as a function of frequency [4]. The sample considered is a high quality, epitaxial, thin (2200 Å) square ($l = 10$ mm) $\text{YBa}_2\text{Cu}_3\text{O}_{7-\delta}$ (YBCO) film, grown by planar high oxygen pressure dc sputtering on a LaAlO_3 substrate [5]. The connection between the cable and the sample is realized through a double-spring method, extensively described elsewhere [6]⁴. The cryomagnetic set-up is a commercial 16 T liquid helium flow cryostat (4–300 K). To reduce the magnetic field at the measuring instrument location, it has been found necessary to place the instrument (Vector Network Analyzer) far enough ($\simeq 2.5$ m) from the magnet, and in addition to keep the field below 9 T. The very long total length of the cable (an additional 1 m is inside the cryostat) has as a drawback a heavy attenuation of the signal, especially at higher frequencies, which prevented us from performing measurements above 35 GHz (well below the cut-off frequency of the cable, that is 50 GHz) and resulted in highly noisy measurements above 20 GHz. This upper frequency limit adds to the lower frequency limit dictated by the unavoidable contact capacitance between the cable and the sample (see also [7], where all the details of the measuring procedure are also reported). In the present case, the capacitance effects were evident up to 6 GHz, so that the actual frequency range over which measurements will be presented in the following of the paper is limited to 6–20 GHz.

⁴ Note that using the notation of that paper $Z_0 = 1/Y_0$.

3. Measurement procedure

The main problem for any frequency-dependent measurement, in the microwave range, is to extract from the measured signal the part due to the sample. In our case, the measured quantity is the reflection coefficient at the instrument location Γ_m , which contains, besides the response of the sample, all the reflections and attenuation that the signal experiences in the cable connecting the sample to the instrument. Due to the very long distance between the measuring instrument and the sample, in general the contribution of the sample to the overall Γ_m is rather small. Further, almost one-third of the line is inside the cryostat, and since the coefficients determining the response of the cable depend on the temperature of each segment of the cable a perfect knowledge of the temperature (and temperature gradient) along the line would be necessary to calculate the contribution of the cable. To overcome this problem, we recently proposed a measurement method [7] which allowed us to detect variations of the real part of the sample resistivity $\Delta\rho(\nu)$ when varying external parameters (such as magnetic field and/or temperature), with no need of a complete knowledge of the cable parameters. The procedure is briefly recalled in the following.

Within the thin film approximation [8], it is possible to demonstrate that the variations of $\rho(\nu)$ are related to the reflection coefficient at the sample surface Γ_0 through the relation

$$\begin{aligned}\Delta\rho(\nu) &= \rho_{H,T}(\nu) - \rho_{H_0,T_0}(\nu) \\ &= Z_0 d \frac{1 - |\Gamma_0(H, T, \nu)/\Gamma_0(H_0, T_0, \nu)|}{1 + |\Gamma_0(H, T, \nu)/\Gamma_0(H_0, T_0, \nu)|}\end{aligned}\quad (1)$$

where d is the thickness of the sample, provided that at least one of the two resistivities verifies the relation $\rho(\nu)d \ll Z_0$ (Z_0 is the characteristic impedance of the vacuum). Further, it is possible to experimentally define a coefficient $\tilde{\Gamma}_m(H, T, \nu)$, obtained from the measured Γ_m and the cable parameters measured at room temperature, which is found to be related to $\Gamma_0(H, T, \nu)$ through a single parameter taking into account the response of the cable: $\tilde{\Gamma}_m(H, T, \nu) \simeq \alpha(T, \nu)\Gamma_0(H, T, \nu)$, so that one can also write

$$\Delta\rho(\nu) \simeq \frac{1 - |\tilde{\Gamma}_m(H, T, \nu)/\tilde{\Gamma}_m(H_0, T_0, \nu)|}{1 + |\tilde{\Gamma}_m(H, T, \nu)/\tilde{\Gamma}_m(H_0, T_0, \nu)|} Z_0 d \quad (2)$$

provided that $T - T_0$ is small enough to ensure $|\alpha(T, \nu)| \simeq |\alpha(T_0, \nu)|$. Equation (2) is the core equation for our procedure for the extraction of the resistivity.

In order to obtain the curve $\rho_{H,T}(\nu)$, it is necessary to use some reference, known, $\rho_{H_0,T_0}(\nu)$ curve, from which the variation can be calculated. To this end, we use the fact that, due to the relatively low sensitivity of this experimental technique, in the absence of magnetic field, ρ can be considered zero a few kelvin below T_c , at any frequency. We then choose $T_0 = 70$ K and $H_0 = 0$ T, and obtain the curve $\rho(\nu; H, T)$ through two separate applications of equation (2). First, we obtain the curve $\rho(\nu; H, T_0) = \rho(\nu; H, T_0) - \rho(\nu; H_0, T_0)$ (having assumed that $\rho(\nu; H_0, T_0) = 0$). Second, $\rho(\nu; H, T)$ is obtained as $\rho(\nu; H, T_0) + (\rho(\nu; H, T) - \rho(\nu; H, T_0))$. We stress that within this procedure the first step is performed using measurements obtained by fixing the temperature and varying the field, while the second step is performed with measurements taken at fixed magnetic field, varying the temperature. In this way, the contribution of the cable is kept as constant as possible between the two measurements used, for each step, to obtain the resistivity differences.

4. Results and discussion

The result of the measuring procedure is reported in figure 1 for $H = 8$ T. We first note that in the normal state the resistivity is expected to be independent of frequency, so that a first test for the

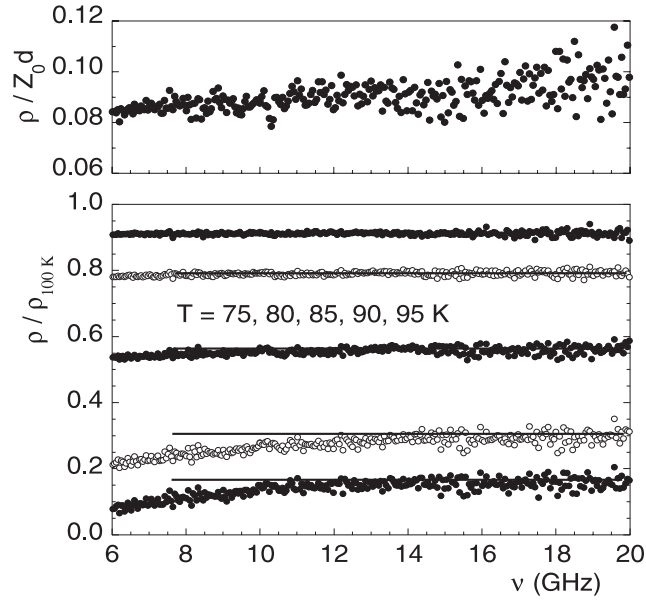


Figure 1. Upper panel: measured $\rho_{8\text{ T}, 100\text{ K}}(\nu)$. As can be seen, the obtained resistivity is almost frequency independent. Lower panel: measured resistivities $\rho_{H,T}(\nu)$ for $H = 8\text{ T}$, normalized to the measurement at 100 K, at different temperatures. Note that the resistivity is constant, as a function of frequency, above $T \simeq 85\text{ K}$.

validity of the measuring procedure is to check whether or not this is obtained experimentally. As can be seen in figure 1 (upper panel), this is reasonably verified for $T = 100\text{ K}$.

The weak frequency dependence can be ascribed to small variations of α with T between $T_0 = 70\text{ K}$ and $T = 100\text{ K}$. It is to be noticed that most of the ‘noise’ seen in the data is due to the cable contribution which is not fully subtracted by the experimental procedure described in [7]. The latter is a systematic signal which is cancelled out when plotting the data at fixed frequency as a function of temperature (see figure 2). To reduce the spurious dependences on ν due to the cable, we define the ratio $R_{H,T}(\nu) = \rho_{H,T}(\nu)/\rho_{H,100\text{ K}}(\nu)$ and plot $R_{H,T}(\nu)$ at 8 T and different temperatures in the lower panel of figure 1. As can be seen, this ratio is much less noisy with respect to ‘raw’ data, allowing for a better definition of the frequency dependence of the resistivity. It is found that R is dependent on frequency only below $T = 85\text{ K}$. This finding can be made more evident by different visualizations of the same data. In figure 2 (main panel) we report $R_{H,T}(\nu)$ at two fixed frequencies (6 and 20 GHz) as a function of temperature, for $H = 2$ and 8 T. As can be seen, at each field the data collapse on a single curve in a reasonably wide temperature range, up to about 110 K, while they are markedly different at lower temperatures, below a rather well defined temperature $T_f(H)$. In order to check that this feature is not due to the variation of the cable response with T , we also report, in the inset, the ratio $\rho_{8\text{ T},T}(6\text{ GHz})/\rho_{8\text{ T},T}(20\text{ GHz})$ for $T < 180\text{ K}$. This ratio is obtained directly through equation (2), without any normalization to the value at 100 K, so that it includes also possible variations of α with T . As can be seen, this ratio is nearly constant over a very wide range of temperatures (about 100 K), and begins to deviate from this value only below the zero-field critical temperature T_{c0} , thus further demonstrating that the variations of α with T are negligible, to our end, in the whole temperature range considered. The finding of different frequency dependences at different temperatures and magnetic fields

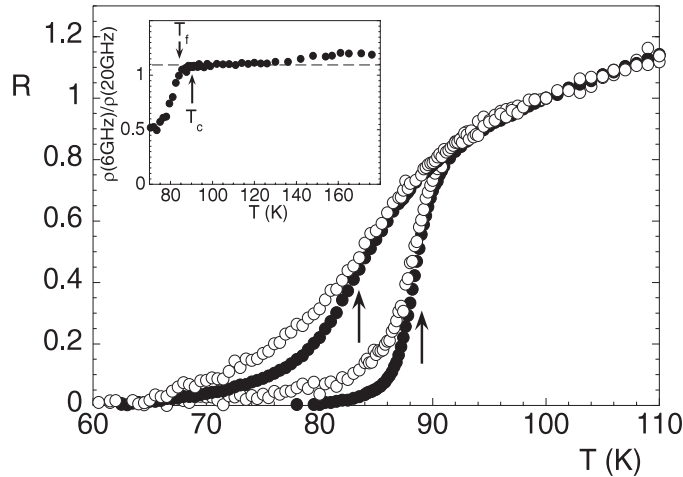


Figure 2. Measured resistivities for $H = 2$ and 8 T, at fixed frequency (6 and 20 GHz) as a function of temperature. Data are normalized to the value at 100 K. The resistivity at the two frequencies is found to be the same down to a well defined temperature, dependent on H (arrows). Inset: ratio $\rho(6 \text{ GHz})/\rho(20 \text{ GHz})$ for $H = 8$ T. The definition of T_f (see text) is extremely precise.

is the main experimental result of this paper, that will allow us to infer that different regimes characterize different regions of the (H, T) phase diagram.

To follow the field variation of this feature, we present in figure 3 the ratio $R_{H,T}(6 \text{ GHz})/R_{H,T}(20 \text{ GHz})$ for several fields, in an enlarged temperature region below T_c . These ratios show a very weak T dependence from around T_c down to a well defined, magnetic field dependent temperature T_f , where the temperature dependence changes abruptly, becoming very strong. This is also seen in the inset of the same figure, where we report different ratios $R_{H,T}(\nu)/R_{H,T}(20 \text{ GHz})$ for $H = 2$ T and $\nu = 6, 10, 16$ GHz. Again, the frequency dependence is very weak above T_f , while it becomes larger and larger below it.

This abrupt change in the frequency dependence across T_f together with its determination as a function of the magnetic field is the second major finding of this paper. It shows that two different dynamic regimes can be directly identified through measurements as a function of frequency. The nature of these two regimes can be understood considering the different dissipative mechanisms present in the HTS: on one hand one has thermal fluctuations, playing a major role near and above the transition temperature, on the other the flux motion, whose contribution becomes dominant at lower temperatures. When studying transport properties at low frequency, the two mechanisms are found to evolve *smoothly* one into the other at intermediate temperatures: according to theories of fluctuations in the presence of an applied magnetic field, the low temperature limit of the expression for the overall dc resistivity coincides in fact with the Bardeen–Stephen expression for the free flux flow [9]. This suggests that from the point of view of (dc) electrical transport properties, it is not possible to distinguish between free flow of vortices and fluctuations.

This framework drastically changes in the presence of disorder. When vortices interact either with pinning centres or with one another, their mobility is limited by these interactions, and the overall resistivity becomes smaller than the free flow expression, eventually reaching a zero value if the interactions are strong enough to completely lock the fluxons. In general, three temperature regions can thus be defined: a region where the disorder does not play a major role, and the dc resistivity can be described either by fluctuational resistivity or free flow

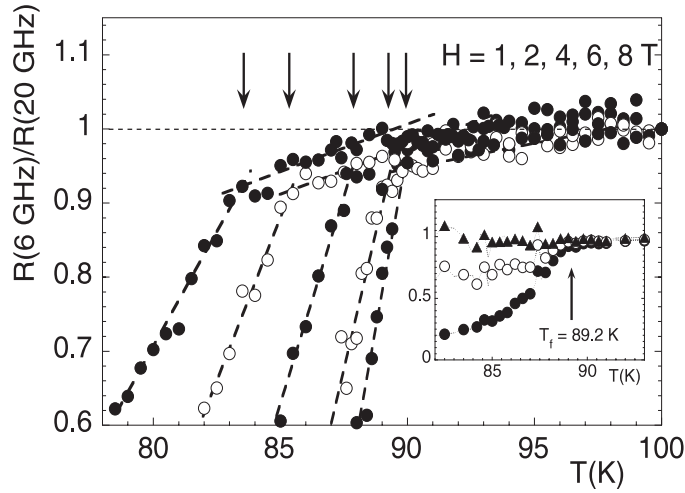


Figure 3. Ratio $\rho(6 \text{ GHz})/\rho(20 \text{ GHz})$ for $H = 1, 2, 4, 6,$ and 8 T . Arrows marks the temperature T_f . Thick lines are guide for the eye. Inset: ratios $\rho(\nu)/\rho(20 \text{ GHz})$ for $\nu = 6$ (full circles), 10 (open circles), and 16 GHz (full triangles) ($H = 2 \text{ T}$).

expressions (free flow/fluctuation regime); a region where the vortices are no longer free to move, but not yet locked (viscous/plastic regime) and a frozen regime in which vortices cannot move over long distances within the sample.

When studying the response of the superconductor as a function of frequency, the three regimes present a clear difference among them: in the free flow/fluctuation regime no dependence on frequency should be present in the frequency range explored by us; the free vortices should not present any frequency dependence, while fluctuations have as a relevant time scale the Ginzburg–Landau time τ_{GL} , which is estimated to be $\tau_{GL} \simeq 30 \text{ fs}$ ($1/\tau_{GL} \simeq 10^5 \text{ GHz}$) or less [11], well outside our experimental window. On the other hand, in the viscous/plastic regime, as well as in the frozen regime, the response of vortices varies sensibly as a function of frequency. For vortices interacting with pinning centres, in fact, it is possible to define a *pinning frequency* ν_p which separates a low frequency regime, in which the vortices cannot follow the electromagnetic stimulus, from a high frequency regime, where vortices are forced to oscillate around their equilibrium positions, thus being able to follow the e.m. stimulus even when strongly pinned. This pinning frequency is estimated to be $\nu_p \simeq 10 \text{ GHz}$ [10]⁵, that is exactly in the frequency range explored by us, so that the response of pinned vortices should result in a large frequency dependence for our data. To quantitatively determine ν_p , it is necessary to identify a reliable model for the vortex dynamics in the presence of generic pinning, which is beyond the scope of this paper. However, independently of the model, it is clear that the pinning frequency becomes less and less defined as the free flow regime is approached: in the free flow regime, in fact, the two dynamical regimes become equivalent and the crossover as a function of frequency can no longer be experimentally identified. Within this general frame, the temperature T_f can thus be identified as the temperature, at a given magnetic field, below which the effect of disorder becomes relevant (the small frequency dependence above T_f can be ascribed to the divergence of τ_{GL} near T_c or to effects due to the quasiparticle

⁵ It is to be noticed that in [10] ν_p is evaluated using the hypothesis of absence of flux creep. This hypothesis might not apply approaching T_c , so that estimations of the T dependence of ν_p at high T through that analysis could be unreliable.

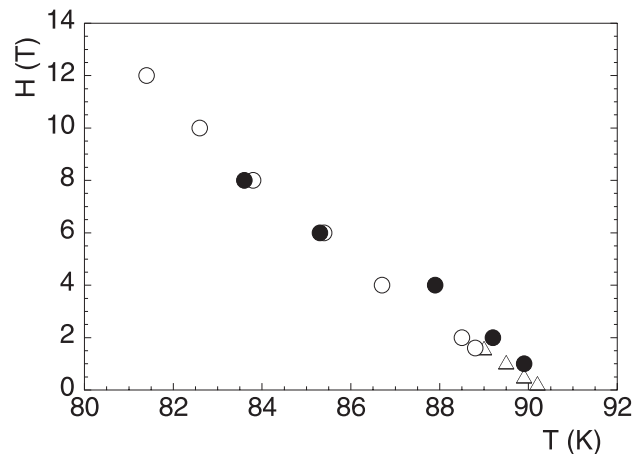


Figure 4. Position of $T_f(H)$ in the (H, T) phase diagram (filled circles). For comparison the values of $T_d(H)$ defined through comparison with fluctuational models in dc (open circles) and through angular scaling (open triangles) are also reported.

contribution, which are not considered in the above discussion). The sharp change of dynamic regime here found should give visible effects on several other independent indicators.

As a first example, we notice that if the effects of disorder are irrelevant, the dc resistivity should follow the predictions of the free flow/fluctuation theoretical models [9]. We have previously found [12] that in YBCO this is actually the case from well above T_c down to a well defined, field dependent temperature $T_d(H) < T_c$. The data for $T_d(H)$ are reported in figure 4 as empty circles. The agreement between T_d and T_f points to a common origin of the two lines. A second important confirmation comes from the angular dependence of the dc resistivity, $\rho_{dc}(T, H, \theta)$. In the absence of directional pinning, given e.g. by the layered structure itself, intrinsic dissipative phenomena (flux flow, fluctuations,...) are expected to scale with the angular dependent upper critical field $H_{c2}(\theta)$. As reported previously [12], in YBCO ρ_{dc} exhibits a clear angular scaling $\rho_{dc}(T, H, \theta) = \rho_{dc}(T, H/H_{c2}(\theta))$, again from a temperature above T_c down to a typical temperature $T_{d,\theta}(H)$. The data for $T_{d,\theta}(H)$ are reported in figure 4 as triangles, and again the same behaviour as T_f is found. It is an important result that all the above reported independent measurements agree extremely well in the determination of a line in the $H-T$ phase diagram, $T_f(H)$, above which extrinsic effects are completely irrelevant in the dynamic properties of the vortex matter. It is seen that the new degree of freedom given by frequency-dependent measurements allows for a direct determination of the change of dynamics, that can only be inferred from dc transport measurements.

5. Conclusions

As a conclusion, we have demonstrated that frequency dependent measurements of the resistivity in HTS are a valuable tool for the study of the dissipative mechanisms. In particular, we have shown that different dynamical behaviour is observed in different T ranges: while at high temperatures and fields the resistivity is found to be nearly frequency independent, at lower magnetic fields and temperatures a strong frequency dependence appear. The crossover between these two regions is found to be rather sharp, so that it is possible to clearly define a magnetic field dependent crossover temperature T_f , which can be obtained directly from the data without the need of any interpretative model. A physical interpretation of these

two regimes has been proposed and verified by the comparison with previous results. In particular, the crossover temperature $T_f(H)$ is found to be coincident with the temperature $T_d(H)$ above which the effects of pinning on vortex lines are found to be irrelevant, which was previously obtained from dc measurements through angular scaling arguments and comparison with fluctuation theory.

Acknowledgment

This work has been partially supported by INFM under project PRA–HOP.

References

- [1] For a review on vortices, see Blatter G, Feigel'man M V, Geshkenbein V B, Larkin A I and Vinokur V M 1994 *Rev. Mod. Phys.* **66** 1125
For fluctuations see Varlamov A A, Balestrino G, Milani E and Livanov D V 1999 *Adv. Phys.* **48** 655
- [2] Sarti S, Fastampa R, Giura M, Silva E and Marcon R 1995 *Phys. Rev. B* **52** 3734
- [3] Banerjee T, Kanjilal D and Pinto R 2002 *Phys. Rev. B* **65** 174521
- [4] Belk N, Oates D E, Feld D A, Dresselhaus G and Dresselhaus M S 1996 *Phys. Rev. B* **53** 3459
- [5] Wu D H, Booth J C and Anlage S M 1995 *Phys. Rev. Lett.* **75** 525
- [6] Beneduce C, Bobba F, Boffa M, Cucolo A M, Cucolo M C, Andreone A, Aruta C, Iavarone M, Palomba F, Pica G, Salluzzo M and Vaglio R 1999 *Int. J. Mod. Phys. B* **13** 1333
- [7] Tosoratti N, Fastampa R, Giura M, Lenzi V, Sarti S and Silva E 2000 *Int. J. Mod. Phys. B* **14** 2926
- [8] Sarti S, Amabile C, Tosoratti N and Silva E 2003 *Preprint cond-mat/0307143*
- [9] Klein M, Chaloupka H, Müller G, Orbach S, Piel H, Roas B, Schultz L, Klein U and Peiniger M 1990 *J. Appl. Phys.* **67** 6940
Silva E, Lanucara M and Marcon R 1996 *Supercond. Sci. Technol.* **9** 934
- [10] Ikeda R, Ohmi T and Tsuneto T 1991 *J. Phys. Soc. Japan* **60** 1051
Ullah S and Dorsey A T 1991 *Phys. Rev. B* **44** 262
- [11] Tsuchiya Y, Iwaya K, Kinoshita K, Hanaguri T, Kitano H, Maeda A, Shibata K, Nishizaki T and Kobayashi N 2001 *Phys. Rev. B* **63** 184517
- [12] Booth J C, Wu D H, Qadri S B, Skelton E F, Osofsky M S, Piqué A and Anlage S M 1996 *Phys. Rev. Lett.* **77** 4438
- [13] Sarti S, Neri D, Silva E, Fastampa R and Giura M 1997 *Phys. Rev. B* **56** 2356
Sarti S, Giura M, Silva E, Fastampa R and Boffa V 1997 *Phys. Rev. B* **55** R6133